

A Comprehensive Study on the Formulation and Evaluation of Neomycin Sulfate-Loaded Transferosome

ALLAM SASIKALA AND G.S ANNAMMADEVI^{1*}

Department of Pharmaceutical Technology, Maharajah's College of Pharmacy, Vizianagaram 535002, ¹GITAM School of Pharmacy, GITAM (Deemed to be University), Visakhapatnam, Andhra Pradesh 530045, India

Sasikala *et al.*: Infused Hydrogel for Effective Topical Management of Vaginal Infections

This research aimed to develop neomycin sulfate-loaded transferosomal vesicles designed for efficient vaginal delivery. The study employed a modified handshaking technique to enhance drug permeability through the vaginal mucosa, utilizing various surfactants at three concentrations while maintaining constant drug concentration. Neomycin sulphate transferosomes were made using a modified hand shaking method and seven different edge activators, which included Brij35, sodium deoxycholate cremophor EL, tween80, span80, and tween20, at three different concentrations of phosphatidylcholine. These formulations were then tested for surface characteristics (scanning electron microscopy and transmission electron microscopy), particle size distribution, zeta potential, differential scanning calorimetry, X-ray diffraction, Fourier transform infrared, small angle X-ray scattering, *ex vivo* permeation studies, and confocal scanning laser microscopy studies. The phospholipid layer's intercalatable surfactant, span80, was used in the formulation process to produce a stable vesicular formulation. The findings showed that the transferosomes loaded with neomycin sulfate were stable, uniformly distributed, and had a particle size of 152.8 nm, a polydispersity index value of 0.368, and a zeta potential of 5.04 ± 0.2 mV. Furthermore, the efficiency of entrapment was 89.87 %. The transferosomes high deformability-a deformability index of 31.8 was validated by the lipid extrusion test. Neomycin sulfate was successfully loaded into vesicles, as demonstrated by additional analysis using differential scanning calorimetry, X-diffract gram patterns, and small angle X-ray scattering studies. These findings suggested that the vesicles were amorphous and that unilamellar vesicles had formed. *In vitro* permeation investigations on sheep vaginal tissue at pH 4.4 citrate buffer indicated promising results for the improved formulation, including a flux value of 0.789 mg/h/cm², a permeability coefficient of 0.0956, a short lag time of 0.434 h, and a 12-fold enhancement ratio compared to pure medication. Confocal laser scanning microscopy investigations validated the vesicles' deformability and improved permeability. In conclusion, neomycin sulfate-loaded transferosomes showed great promise as a drug delivery technology for vaginal applications. The proposed vesicular formulation demonstrated superior properties such as stability, deformability, and increased permeability, making it a promising carrier with fewer side effects and the possibility for easy scale-up and production at lower medication doses.

Key words: Small angle X-ray scattering, unilamellar structure, Fourier transform infrared, X-ray diffraction

Bacterial *Proteus* infections are vaginal infections caused by the *Bacillus proteus* (*B. proteus*) microorganisms. This species is widely recognized for its resistance to treatment, and infections associated with it have not responded well to streptomycin, antibiotics, or chemotherapeutic drugs. Weinberg *et al.*^[1] investigated and reported on the numerous treatment options available for *B. proteus* infections.

The structure of transferosome vesicles is distinct;

they are colloidal particles with a water-filled core encircled by a bilayer of lipids and surfactants (amphiphiles). Amphiphiles have the ability to form one or more concentric bilayers when the

This is an open access article distributed under the terms of the Creative Commons Attribution-NonCommercial-ShareAlike 3.0 License, which allows others to remix, tweak, and build upon the work non-commercially, as long as the author is credited and the new creations are licensed under the identical terms

*Address for correspondence
E-mail: mannam@gitam.edu

Accepted 29 October 2024
Revised 20 June 2024
Received 05 December 2023
Indian J Pharm Sci 2024;86(5):1883-1893

proportion of water is increased. This allows the hydrophilic drug to be encapsulated within the aqueous compartment, while lipophilic drugs and amphiphiles become trapped in the bilayer wall due to hydrophobic forces. IDEAA AG, Munich, Germany claims that transferosomes, also referred to as "deformable liposomes, ultra deformable liposomes, flexible liposomes, ultra-flexible liposomes, 2nd generation vesicles", outperform conventional drug delivery systems in terms of bioavailability and have fewer harmful side effects^[2]. Transferosomal composition was found to be biocompatible with the biological cell membrane by Bibi *et al.*^[3] and Kumavat *et al.*^[4], meaning that they can be employed for the administration of all drug classes. The stability and permeability of transferosomal vesicles are determined by the type and amount of Edge Activator (EA) to phospholipid ratio^[5].

MATERIALS AND METHODS

Bulk medications, chemicals, and reagents:

Yarrow Chem., Bangalore is the source of Neomycin Sulfate (NS) (fig. 1a). Gift samples from Strides Pharma included Egg Phosphatidylcholine (EPC) (fig. 1b), Brij 35, span20, Tween 20, tween80, span80 (fig. 1c), and cremophor EL. Sodium deoxycholate was bought from Thermo Fischer Scientific India Pvt. Ltd., Every ingredient, reagent, and excipient complies with pharmaceutical standards.

Procedures:

Formulation of neomycin sulphate loaded transferosomes: The production of NS-loaded transferosomes was accomplished through a modified handshaking method that involved the use of seven distinct EA, namely Brij35, sodium deoxycholate

cremophor EL, tween80, span80, tween20, and tween80, at three distinct ratios of phosphatidylcholine to EA: 17:3, 9:1, and 19:1. In summary, necessary concentrations of lipid and surfactant were dissolved in a 3:1 ethanol to chloroform organic solvent mixture and agitated for a duration of 1 h. In order to completely evaporate the remaining solvent, the solvent was evaporated until a thin layer formed at the bottom of the beaker, which was then placed in the desiccator for the entire night. For additional research, the medication (5 mg) was dissolved in 4.4 pH citrate buffer and put onto the dry films. The films were then sonicated for 15 min and kept between 4° and 8°.

Transferosomes loaded with NS characterization^[6]:

Measurement of turbidity: Using Nephelometry, turbidity was assessed for each prepared NS transferosomal suspension. This is a crucial factor in choosing the best formulation.

Measurement of vesicle count: NS loaded Transferosomal formulation was diluted with 0.9 % Sodium chloride (NaCl) solution, put on a hemocytometer, and the number of vesicles was measured ($\times 100$).

Total no. of transferosomes per cu.mm = Total number of transferosomes counted \times dilution factor $\times 4000$ / total number of squares counted.

Measuring the drug-loading efficiency of vesicles:

Vanden *et al.*^[7] approach was used to measure the prepared transferosomes loading efficiency.

The total drug was determined by the following formula:

Loading efficiency % = Total drug-free drug / total drug $\times 100$

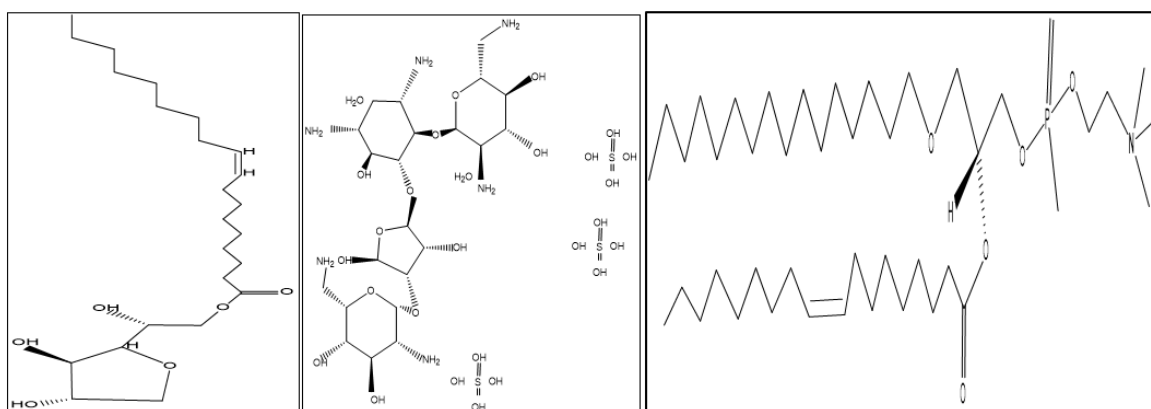


Fig. 1: Structure of span80, neomycin sulphate and egg phosphatidylcholine

Determination of surface charge on vesicles:

Malvern instruments were used to determine the zeta potential (mV), which allowed for the measurement of the surface charge on each vesicle.

Homogeneity index and Particle Size Distribution (PSD): Using Dynamic Light Scattering (DLS) and Malvern Instruments Ltd., the size of the particle and heterogeneity index of the produced transferosomes were ascertained.

Deformability nature: The liposofast lipid extruder EVOKO 3040/580 was used to determine the deformability nature. Using a method described by Gillet *et al.*^[8], Cevc *et al.*^[9] and Jain *et al.*^[10], a vesicular suspension of known particle size was passed through a polycarbonate membrane with a pore size of 50 nm and extruded through under 500 psi for three cycles. The volume of suspension collected was measured, and the deformability index was calculated.

Ex vivo penetration assays and their specifications:

A Franz diffusion cell with vertical diffusion assembly (NSIL, Lab Works Pvt. Ltd.) with a receiver compartment volume of 25 ml and an effective diffusion area of 2.33 cm² was used for permeability tests, and citrate buffer (pH 4.4) was used. Research reporters have claimed that the best model for evaluating vaginal formulations is sheep vaginal tissue, supporting that statement *in vitro* drug permeation study was conducted using reported method^[11-14]. Mature sheep's vaginal tissue was collected from slaughter house, removed and preserved in regular saline solution. 25 ml of citrate buffer (pH 4.4)^[15] was added to the receptor compartment, which was kept at 37[°]±0.5[°] and rotated at 270 rpm using a magnetic bar.

Formulations (corresponding to a 3 mg drug) were applied to the skin, and it was placed on diffusion cell receptor compartment. To maintain sink conditions, 2 ml aliquots of the receptor medium were taken out at the proper intervals and quickly replaced with an equal volume of citrate buffer (pH 4.4). The data on permeation profiles were calculated taking into account correction factors for every aliquot. Ultraviolet (UV) was used to analyze the aliquots. The steady-state flux (J_{ss} , expressed as mg/h/cm²), lag time, and permeability coefficient values (K_p) were the *ex vivo* permeation parameters that needed to be calculated. The slope value, which is obtained by graphing the relationship between time and the cumulative amount of drug permeated ($\mu\text{g}/\text{cm}^2$) per unit area, equals the steady-

state flux (J_{ss} , expressed as mg/h/cm²)^[16]. Permeability coefficient is obtained by calculating dividing flux to total amount of drug taken initially on to donor compartment membrane's surface.

Lyophilization of the optimal formulation:

Using a freeze dryer (model Alpha 1-2 CD plus equipped with vacuum pump system Telastar 2G-6, Spain) at 0.005 mbar, liquid nitrogen was used to lyophilize the optimized NS-loaded transferosome and the plain transferosome at -80[°].

Scanning Electron Microscopy (SEM) analysis:

Using carbon-based adhesive tape, a small amount of the Lyophilized Product (LP) was deposited on a glass slide that was placed over the grid. Using a high vacuum pump and at a voltage of 30 kV, the gold-palladium-coated vesicles were imaged using SEM A071020 (2 l, CarlZeiss, Brighton, Germany).

Transmission Electron Microscopy (TEM) analysis:

The formulation was spread out on a 400 mesh copper grid coated in carbon, stained with a drop of 1 % phosphotungstic acid solution, and allowed to air dry. A voltage of 200 kV was used to accelerate the photomicrographs.

Differential Scanning Calorimetry (DSC):

Using a nitrogen gas purging flow rate of 30 ml/min in the DSC Q-100 apparatus (TA instruments, UK), the lyophilized formulation was put on an aluminum pan and subjected to temperature ranges between 30[°]-270[°] at a rate of 10[°] per minute.

X-Ray Diffraction (X-RD) studies:

The Bruker D2 phaser model, equipped with a LynxEye detector, was used to measure diffraction. The generator's working voltage was set at 30 kV and 10 mA. The X-ray source consists of Cu enclosed in sealed tubes, which generates monochromatic radiation from graphite (display wavelength=1.5406Å) with a goniometer radius of 141 mm. The range of the data depicted in the angular pattern was 3.0020<2θ<40.0050.

With a step size of 0.0120, the diffractograms were captured at a total of 72.60 s per step. In order to minimize the impact of preference orientation and obtain the optimal peak for analysis, the samples were rotated. They were placed on an inclined crystal to reduce background interference caused by the vitreous support.

Fourier Transform Infrared (FTIR) studies:

H-bonds between phospholipid head groups and interfacial water molecules can be identified and phospholipid membrane chemical information can be obtained using FTIR spectroscopy^[17]. Additionally, the temperature dependence of various vibrational modes resulting from structural changes makes FTIR a perfect tool for studying the melting behavior of lipid membranes and provides a complete means of monitoring phase transitions. Drug compatibility with transferosomal components is assessed using FTIR spectroscopy. (Agilent Technologies, United States of America (USA); Cary, 630 model) for transferosomal formulation, physical mixtures, constituents in formulations, and pure drugs, it was noted.

Small Angle X-Ray Scattering (SAXS):

The SAXS space model (Anton par) was used to calculate SAXS investigations for plain vesicles, 4.4 pH citrate buffer^[18], and optimized NS-loaded transferosomal vesicles. Following a 15 min period of sonication, the suspension was passed through 0.45 mm filters. The transferosomal suspension was then placed into glass capillaries measuring 2 mm in diameter and sealed for additional examination at room temperature in a vacuum.

Confocal laser scanning microscopy:

The purpose of this experiment was to determine the depth of penetration of the vaginal mucosal tissue by the optimized NS-S80. Using Rhodamine B, a hydrophilic dye (0.01 % of 20 µl), optimized transferosomal vesicles were rendered fluorescent during production and subsequently applied to sheep vaginal tissue mounted on Franz diffusion cells. Following 7 h of penetration testing, the permeated region was removed by cutting and quickly frozen at -80°. Using a cryostat microtome (Micro HM 560, Bio-Optica, Milan, Italy), thin slices of vaginal tissue were created for a permanent slide transverse section longitudinally. These slices were then examined using immersion oil pictures and confocal laser scanning microscopy at various depths of the vaginal mucosal layers.

RESULTS AND DISCUSSION

To generate NS-loaded transferosomes, a modified handshaking approach was used, utilizing three different quantities of sodium deoxycholate, tween80, span80, tween20, and span20, as well as Cremophor EL and brij35. Turbidity (measured in NTU units), vesicle count, loading efficiency, Zeta potential, PSD, and Polydispersity Index (PDI) were assessed for the manufactured transferosomes as shown in Table 1.

TABLE 1: MEAN TURBIDITY, MEAN VESICLES PER CUBIC MILLIMETER, PERCENT ENTRAPMENT EFFICIENCY, DRUG PAY LOAD, ZETA POTENTIAL, PSD AND POLY DISPERSIBILITY INDEX RESULTS OF NEOMYCIN SULPHATE LOADED TRANSFEROSOMES (n=3)

Formulation code	EA	PG: EA	Turbidity ^b (NTU)	No. of vesicles/mm ³	Loading efficiency (%)	Drug Pay load	ZP (mV)	PSD (nm)	PDI
NS S80 (a)		95:5	24	51	83±0.37	4.36	3.71±0.11	239.6±0.61	0.398±1.1
NS S80 (b)	Span80	90:10	32	49	87±1.32	4.83	3.89±0.13	251.7±0.79	0.389±1.8
NS S80 (c) ^a		85:15	36	44	89.8±0.87	5.35	5.04±0.02	152.3±0.58	0.379±2.5
NS T80 (a)		95:5	8	39	52±0.77	2.73	0.229±1.3	189.4±1.1	0.393±0.51
NS T80 (b)	Tween80	90:10	10	30	55±0.54	3.05	0.249±1.5	171.3±1.7	0.382±0.45
NS T80 (c)		85:15	19	26	59±0.69	3.47	0.264±2.1	152.3±2.1	0.368±0.63
NS B35 (a)		95:5	16	25	43±0.69	2.26	2.25±0.70	191.5±2.5	0.432±0.23
NS B35 (b)	Brij 35	90:10	19	20	45±0.88	2.5	2.49±0.59	177.3±1.8	0.419±0.04
NS B35 (c)		85:15	24	12	49±0.79	2.98	2.63±0.13	168.5±1.7	0.396±0.19
NS SDC (a)		95:5	12	27	48±0.94	2.52	1.31±1.80	169.8±2.4	0.398±2.3
NS SDC (b)	Sodium deoxycholate	90:10	18	21	50±0.61	2.77	1.50±1.50	151.3±1.5	0.387±1.7
NS SDC (c)		85:15	24	18	55±0.59	3.23	1.62±1.70	136.4±2.8	0.374±2.4
NS S20 (a)		95:5	21	46	75±0.49	3.94	0.443±0.55	235.3±0.41	0.351±0.89
NS S20 (b)	Span20	90:10	29	44	79±0.90	4.38	0.459±0.69	220.1±0.59	0.339±0.71
NS S20 (c)		85:15	31	40	84±0.6	4.94	0.467±0.78	203.8±0.45	0.316±0.91

NS T20 (a)		95:5	19	31	44±0.87	2.31	-1.13±0.74	281.3±0.42	0.423±0.11
NS T20 (b)	Tween20	90:10	22	26	46±0.67	2.55	-1.25±0.0.83	262.4±0.59	0.411±0.39
NS T20 (c)		85:15	24	21	51±0.71	3	-1.32±0.59	242.3±0.70	0.395±0.25
NSCEL (a)		95:5	24	36	61±0.67	3.21	2.71±0.19	185.6±0.91	0.298±0.51
NSCEL (b)	Cremophor EL	90:10	32	33	66±0.76	3.66	2.89±0.25	167.2±0.61	0.289±0.49
NSCEL (c)		85:15	19	31	69±0.85	4.05	3.02±0.39	143.5±0.54	0.278±0.31

Note: ^aOptimized formulation loaded with neomycin sulphate and ^bStandard deviation to mean was present to the fourth decimal

As shown in Table 1, the turbidity and vesicle count values of all 21 formulations fall between 8 and 36 NTU and 12 and 51 vesicles/mm³. Compared to all the other formulations, Formulation NS S80 (c) showed the highest turbidity and vesicle count. In comparison to the other two levels, all 85:15 PG: EA formulations showed increased turbidity and vesicle count. This may be explained by the increased edge-activator concentration. However, the findings of the formulation with Cremophor EL were different.

According to Table 1, the results for all 21 formulations show that their respective loading efficiency and drug pay load fall between 43±0.69 %, 89.8±0.87 % and 2.26 %, 5.35 %. Among all the formulations, formulation NS S80 (c) demonstrated the highest loading efficiency and drug pay load. Both the loading efficiency and the drug payload increased when the EA concentration rose in each formulation. The Surface charge on the vesicles, PSD, and PDI of each prepared NS transferosome were assessed; Table 1 shows the results. The vesicle's surface charge was measured to be between -1.32±0.59 and 5.04±0.02, while the PSD and PDI were determined to be between 152.3 and 281 nm and 0.278 and 0.423, respectively. Out of all the formulations, NS S80 (c) showed a PSD of 152.6 and a surface charge of 5.04±0.02. According to Derjaguin-Landau-Verwey-Overbeek (DLVO) theory there must be steadiness between Vander Waal forces and electrical repulsive forces. Positive zeta-potential values of vesicles do not claim any harmful effect, so as Negative charged vesicles will do so. Every formulation's PDI was determined to be less than 1, showing consistency in the size of the vesicles. It was found that the vesicle particle reduced in all formulations when the concentration of the EA increased. The decrease in interfacial tension between the transferosomal vesicles may be the cause of this. With a poly-dispersibility index of 0.379, NS-S80c demonstrated the highest level of stability across all the formulations. When Span80 is compared to other surfactants, it is found that it's ordered hydrophobic chain is better suited for the drug's entrapment into

an aqueous compartment. A phospholipid layer's extremely disorganized structure allows the medicine to be more fully entrapped in the aqueous compartment of a water-loving molecule. According to Quaglia *et al.*^[19], large molecule or polymer coatings have the ability to shift the plane of shear further away from the particle surface. Sometimes, this could result in a lower zeta potential. Even with relatively lower zeta values, the formulation may be more stable. Strong electrostatic contact with mucus or negatively charged mucosal surfaces is said to result from a positive zeta-potential value, eventually favoring cell mucosal adhesion NS-S80c was therefore optimized for additional research^[20-22]. The elastic and deformable properties of the improved formulation were assessed. As shown in fig. 2, the improved formulation's particle size, PDI, and zeta-potential were compared before and after deformability. B and C after 5 min, 6.8 ml of suspension were collected, with a particle size of 136 nm and a deformability index value of 31.8. To formulate transferosomes, a high deformability index is required. As a result, span80 showed greater vesicle deformability. Better permeability was obtained from NS-loaded transferosomes that were optimized with span80. The presence of ethanol further improves vesicle penetration through mucus and the vaginal mucosa membrane. For NS and NS S80c, the total amount of medication that permeated in 24 h was found to be 225 µg/cm² and 281 µg/cm², respectively; fig. 2 shows this data. The improved formulation's flux was found to be 0.789 mg/h/cm², its permeability coefficient was found to be 0.0956 with a short lag time of 0.434 h, and the enhancement ratio between the pure drug and the NS-loaded transferosomes was found to be 12 times higher.

As shown in fig. 3 and fig. 4, the optimized transferosomes were evaluated for SEM and TEM examination. Pictures of a lyophilized mixture of loaded and unloaded vesicles confirm that the vesicles have a circular form, and their sizes match the information on the PSD. Within the nanoscale range PSD, spherical vesicles were detected by the

TEM pictures. At 221°, NS showed an endothermic peak. The DSC investigations showed that, as shown in fig. 5, the lack of the drug peak might be caused by either molecular drug dispersion in vesicles in an amorphous state or by NS being trapped in vesicles. Table 2 and fig. 6 have showed the acquired summary of X-Rd peaks. The distinctive peaks of the optimized formulation, S80, EPC, physical combination, and NS are shown in fig. 7. The stretching of NH, OH, and CH (aromatic) was responsible for the FTIR bands of NS at 3451 cm⁻¹, 3749 cm⁻¹, and 2342.6 cm⁻¹. The stretching of C=C and C-H was represented by bands

of 1522.6 cm⁻¹ and 3885.7 cm⁻¹, and the stretching of C-O and C=O was represented by bands of 1625.8 cm⁻¹ and 1021.3 cm⁻¹. Peaks at 1737.55 cm⁻¹ (C=O stretching) and 3438.46 cm⁻¹ (O-H stretching) were visible in the span80 spectra. At 3438.46 cm⁻¹, the board peak revealed an intermolecular hydrogen bond. The final optimized formulation (NS S80c) has no substantial incompatibility, according to the FTIR spectra, which also showed that pure NS and chosen additives are compatible. Table 3 contains the tabulated FTIR peaks. SAXS

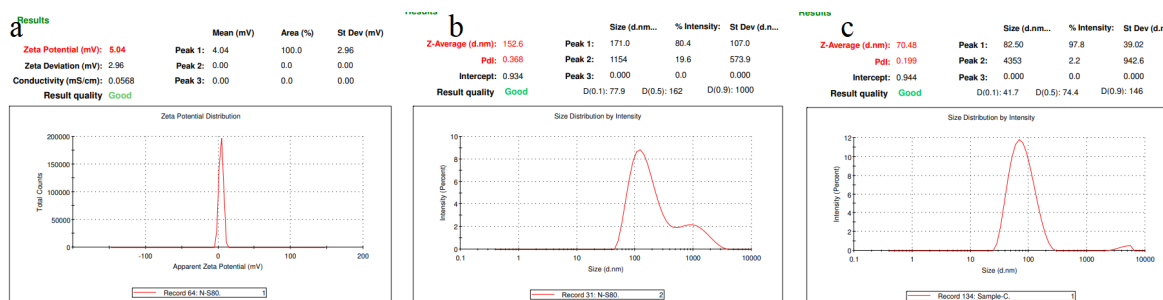


Fig. 2: (A): Zeta potential of optimized formulation (NS S80c); (B) PDI and PSD of Ns S80c and (C): PDI and PSD of NS S80c after lipid extrusion test

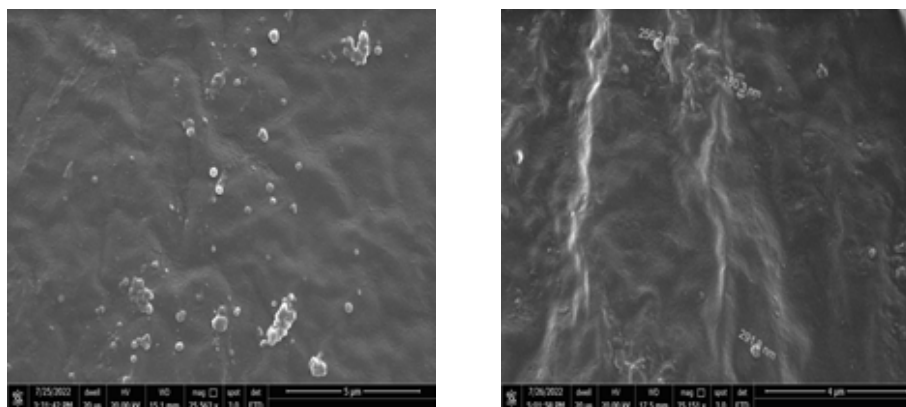


Fig. 3: Scanning electron microscopic images, (a): Freeze dried nanosuspension (without drug) and (b): Freeze dried nanosuspension of optimised formulation (nss80c) at magnification of 25, 563 and 35, 151 respectively

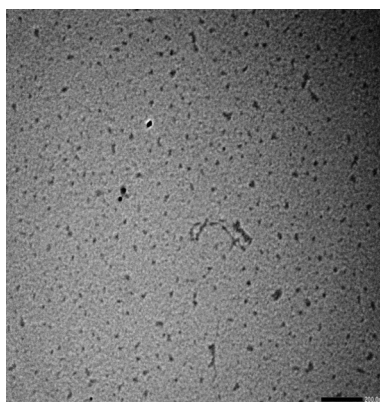


Fig. 4: Transmission electron microscopic images of optimised formulation (NSS80C) at 200 nm scale

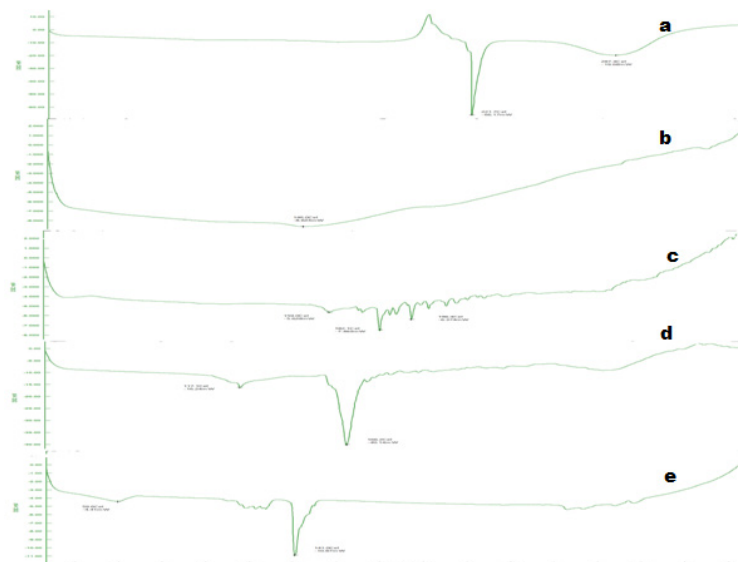


Fig. 5: DSC thermogram, (A): Neomycin sulphate; (B) EPC; (C): S80 and (D): Physical mixture and (E): NSS80C freeze dried form

TABLE 2: SUMMARY OF DSC SCREENING FOR IDENTIFICATION OF NEOMYCIN SULPHATE TRANSFEROSOMES

Moiety	Endotherm (°)	Inference
Neomycin sulphate	221.7	Stable form of neomycin sulphate
EPC	35 182.1, 196.4	Glass transition peak Crystalline state of fatty acid part of EPC
Physical mixture	50.6, 141.3	Little variation in enthalpy changes, no significant interaction
Freeze dried product	117.1, 166.2	Glass transition temperature of lipid and molecular dispersion of drug

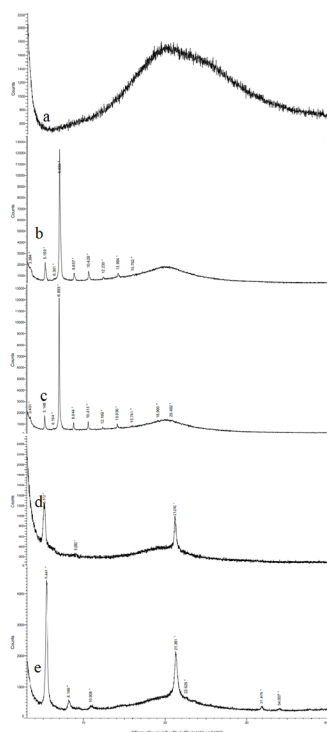


Fig. 6: (a): X-RD spectra neomycin sulphate (b): Egg phosphotidylcholine; (c): Neomycin sulphate/egg phosphotidylcholine (physical mixture); (d) Optimized formulation plain transferosomes. Without drug for freeze dried product and (e): Freeze dried product of optimized transferosomal suspension (NS S80C)

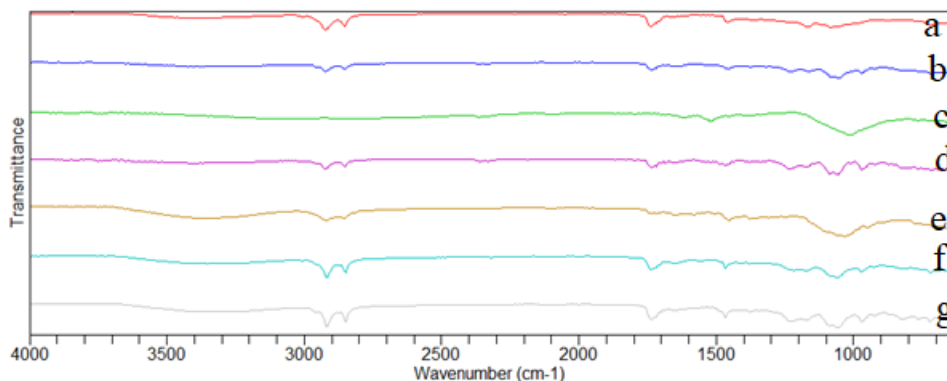


Fig. 7: FTIR of (a): SPAN80; (b): Physical mixture of NS//EPC/S80; (c): Neomycin sulphate; (d): EPC; (e): Optimized formulation in transferosomal suspension form; (f): Plain transferosomes without drug in freeze dried nanosuspension form and (g): Freeze dried nanosuspension of optimized formulation (NSS80C)

TABLE 3: SUMMARY OF FTIR PEAKS

Functional groups (Neomycin sulphate)	Observed wave no. (cm ⁻¹)
Neomycin sulphate	
-NH Stretching	3451.5
-OH Stretching	3749.7
-CH (aromatic)	2342.6
-C=C bond	1522.6
-C-H bond	3904.4
-C-O bond	1522.6
-C=O bond	1021.3
Functional groups (SPAN80)	
OH	3445.9
CH ₂ (Symmetric)	2924.1
CH ₂ (Symmetric)	2853.3
C=O	1735.1
C=C	1654.9
C-H	1459.3
-C-O	1167.5
Functional groups (Egg phosphotidylcholine)	
OH	3445.9
CH ₂ (Symmetric)	2924.1
CH ₂ (Symmetric)	2853.3
C=O	1735.1
C=C	1654.9
C-H	1459.3

-C-O	1167.5
Neomycin sulphate in transferosomal suspension form	
N-NH Stretching	3613.7
OH Stretching 1)	3749.7
CH (aromatic) (cm-1	2361.3
-C=C bond	1541.3
C-H	3867.1
C=O	1082.8
Neomycin sulphate (optimized formulation) NS S80 c LP	
-NH Stretching	3367
CH Stretching	2922
CH (alkane)	2855.1
-C=C bond	1845
C-H	1792.8
C=O	1718.3
C=O	1735.4
CH (aromatic)	1682.9
-NH stretching	3367

by plotting the scattering vector on the X-axis and the scattering intensity on the Y-axis, small-angle SAXS graphs were created. The fundamental plot known as the Guinier plot (fig. 8) illustrates the structure and interparticle interactions of the nanoparticles in prepared colloidal dispersions. The SAXS profiles of buffer, loaded, and plain vesicles are shown in fig. 9. Sharp diffuse scattering curves showed that the vesicles were of multilamellar structure for buffer, loaded (NSS80c) formulation, and plain vesicles without drug. However, there was little difference in the intensity of the loaded and plain vesicles and a greater intensity peak was observed with the NS loaded transferosomal formulation, which may have been caused by the vesicles' increased diameter. Owing to presence of Span80, the intensity of the small angle SAXS curve in plain transferosomes decreases, with the q value centered at 0.08 nm^{-1} for loaded transferosomes. For loaded transferosomes, the q value centered at 0.09 nm^{-1} indicates an increase in intensity, which may be the result of some vesicle disorder following drug loading into a hydrophilic compartment in the vesicle. For big scattering angles, the graph between the scattering vector and $q^4 I(q)$ in fig. 9 is a porods plot.

A scattering curve was produced for both the loaded and plain vesicles (NSS80c) since the NS-laden transferosomes were larger than 265 nm, as shown by the PSD and PDI data. The sheep vaginas that were removed were used for the Confocal Scanning Laser Microscopy (CSLM) research. Fig. 10 shows pictures from CSLM research done on the tissue, revealing the transferosomes' pliable nature and capacity for penetration. The degree of penetration into the underlying tissues is shown by the intense green glow. Fig. 10 CSLM loaded an improved transferosomal formulation (NS-S80c) with dye (Rhodamine B-1 %). In conclusion, the physicochemical features of Neomycin-loaded transferosomes are influenced by the ratio of phospholipids to surfactants and the kind of surfactant, particularly with regard to entrapment efficiency, zeta-potential, PSD, and PDI. The synthesized transferosomes loaded with NS were evenly distributed, stable at a zeta-potential of +5 mV, and had an excellent penetration rate. The particles had a size of 152.8 nm, a PDI of 0.368, this high PDI is frequently observed in vesicles made using a thin-film hydration technique, and an entrapment efficiency of 89.87 %^[23].

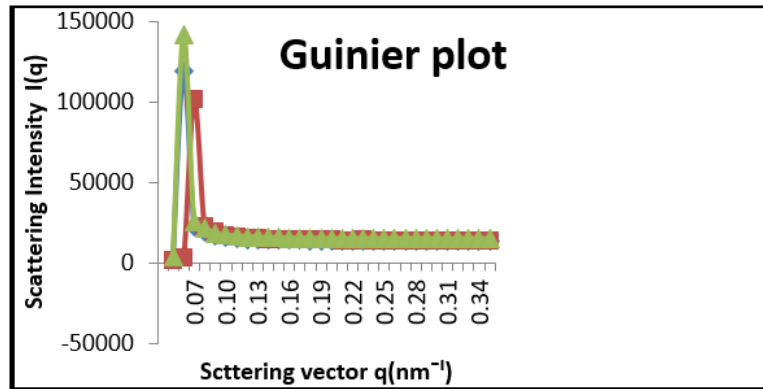


Fig. 8: Guinier plot

Note: (—◆—): Buffer; (—■—): Plain transferosomes and (—▲—): Drug loaded vesicles

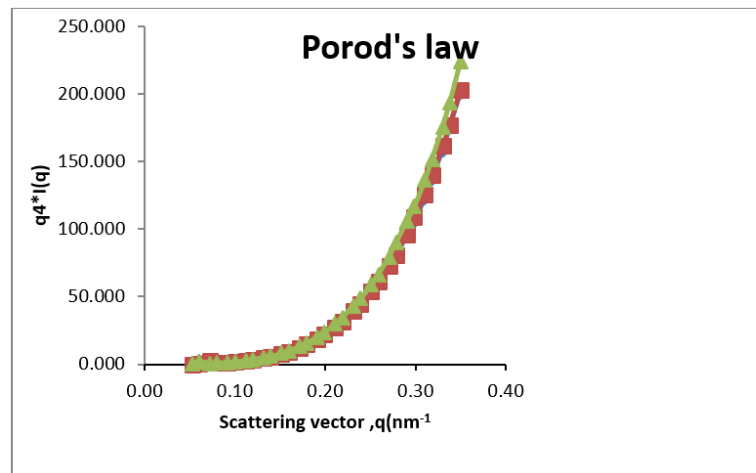


Fig. 9: Porod's graph

Note: (—◆—): Buffer; (—■—): Plain transferosomes and (—▲—): Drug loaded vesicles

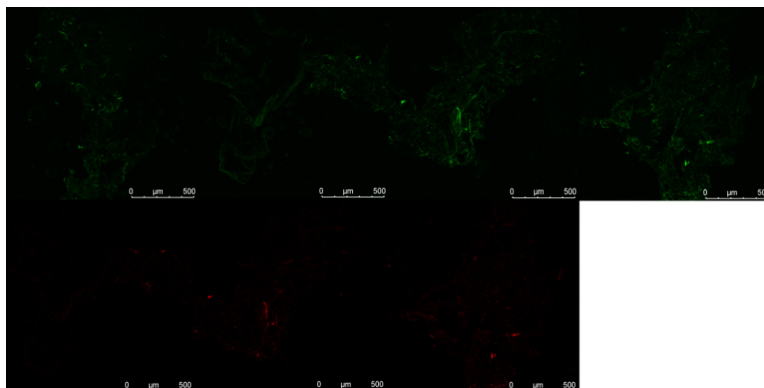


Fig. 10: CSLM after applying dye (rhodamine B-1 %) loaded optimized transferosomal formulation (NS-S80C)

Acknowledgements:

The authors are thankful to Maharajah's College of Pharmacy, Vizianagaram, India and GITAM Institute of Pharmacy, Visakhapatnam, India for supporting and providing necessary facilities for the research work.

Funding:

This research did not receive any specific grant from

funding agencies in the public, commercial, or not-for-profit sectors.

Conflict of interests:

The authors declared no conflict of interests.

REFERENCES

- Weinberg WE. Topical neomycin in cervical and vaginal infections with special reference to *Bacillus proteus* infections. S Afr Med J 1955;29(1):14-6.

2. El Zaafrany GM, Awad GA, Holayel SM, Mortada ND. Role of edge activators and surface charge in developing ultra-deformable vesicles with enhanced skin delivery. *Int J Pharm* 2010;397(1-2):164-72.
3. Bibi N, Ahmed N, Khan GM. Nanostructures in transdermal drug delivery systems. *Nanostruct Drug Deliv* 2017; 639-68.
4. Kumavat SD, Chaudhari YS, Borole P, Duvvuri P, Buberana N, Shenghani K, *et al.* Transfersomes: A promising approach for transdermal drug delivery system. *Asian J Pharm Sci Res* 2013;3(5):1-7.
5. Ascenso A, Salgado A, Euletério C, Praça FG, Bentley MV, Marques HC, *et al.* *In vitro* and *in vivo* topical delivery studies of tretinoin-loaded ultra-deformable vesicles. *Eur J Pharm Biopharm* 2014;88(1):48-55.
6. Jain S, Jain P, Umamaheshwari RB, Jain NK. Transfersomes-A novel vesicular carrier for enhanced transdermal delivery: Development, characterization, and performance evaluation. *Drug Dev Ind Pharm* 2003;29(9):1013-26.
7. van den Bergh BA, Vroom J, Gerritsen H, Junginger HE, Bouwstra JA. Interactions of elastic and rigid vesicles with human skin *in vitro*: Electron microscopy and two-photon excitation microscopy. *Biochim Biophys Acta* 1999;1461(1):155-73.
8. Gillet A, Grammenos A, Compere P, Evrard B, Piel G. Development of a new topical system: Drug-in-cyclodextrin-in-deformable liposome. *Int J Pharm* 2009;380(1-2):174-80.
9. Cevc G, Schatzlein A, Richardsen H. Ultra-deformable lipid vesicles can penetrate the skin and other semi-permeable barriers unfragmented. Evidence from double label CLSM experiments and direct size measurements. *Biochim Biophys Acta* 2002;1564(1):21-30.
10. Jain S, Tiwary AK, Sapra B, Jain NK. Formulation and evaluation of ethosomes for transdermal delivery of lamivudine. *AAPS Pharm Sci Tech* 2007;8:249-57.
11. Mehta S, Verstraelen H, Peremans K, Villeirs G, Vermeire S, de Vos F, *et al.* Vaginal distribution and retention of a multiparticulate drug delivery system, assessed by gamma scintigraphy and magnetic resonance imaging. *Int J Pharm* 2012;426(1-2):44-53.
12. Moss JA, Malone AM, Smith TJ, Kennedy S, Kopin E, Nguyen C, *et al.* Simultaneous delivery of tenofovir and acyclovir *via* an intravaginal ring. *Antimicrob Agents Chemother* 2012;56(2):875-82.
13. Vincent KL, Bourne N, Bell BA, Vargas G, Tan A, Cowan D, *et al.* High resolution imaging of epithelial injury in the sheep cervicovaginal tract: A promising model for testing safety of candidate microbicides. *Sex Transm Dis* 2009;36(5):312-8.
14. Krausit P, Sarisuta N. Development of triamcinolone acetone-loaded Nanostructured Lipid Carriers (NLCs) for buccal drug delivery using the Box-Behnken design. *Molecules* 2018;23(4):982.
15. Lee CH, Chien YW. *In vitro* permeation study of a mucoadhesive drug delivery system for controlled delivery of nonoxynol-9. *Pharm Dev Technol* 1996;1(2):135-45.
16. Ruela AL, Perissinato AG, Lino ME, Mudrik PS, Pereira GR. Evaluation of skin absorption of drugs from topical and transdermal formulations. *Braz J Pharm Sci* 2016;52(03):527-44.
17. Mbah CC, Builders PF, Attama AA. Nanovesicular carriers as alternative drug delivery systems: Ethosomes in focus. *Expert Opin Drug Deliv* 2014;11(1):45-59.
18. Machado RM, Oliveira A, Gaspar C, Oliveira J, Oliveira R. Studies and methodologies on vaginal drug permeation. *Adv Drug Deliv Rev* 2015;92:14-26.
19. Quaglia F, Ostacolo L, Mazzaglia A, Villari V, Zaccaria D, Sciortino MT. The intracellular effects of non-ionic amphiphilic cyclodextrin nanoparticles in the delivery of anticancer drugs. *Biomaterials* 2009;30(3):374-82.
20. Makhlof A, Werle M, Tozuka Y, Takeuchi H. A mucoadhesive nanoparticulate system for the simultaneous delivery of macromolecules and permeation enhancers to the intestinal mucosa. *J Control Release* 2011;149(1):81-8.
21. Sasikala A, Annammadevi GS. Formulation and characterization of triamcinolone acetone loaded transfersosomal vesicles: An attempt for solubility and permeability enhancement for its vaginal delivery. *Res J Pharm Technol* 2024;17(7):3297-304.
22. Sasikala A, Annammadevi GS. Transfersomes-A new transformation in research: A Review. *J Sci Res Rep* 2024;27(9):56-105.
23. Salama AH, Aburahma MH. Ufasomes nano-vesicles-based lyophilized platforms for intranasal delivery of cinnarizine: Preparation, optimization, *ex vivo* histopathological safety assessment and mucosal confocal imaging. *Pharm Dev Technol* 2016;21(6):706-15.